Preprints of the 19th World Congress
The International Federation of Automatic Control
Cape Town, South Africa. August 24-29, 2014

Karhunen Loeve basis used for Detection of Gearbox Faults in a Wind Turbine

Peter Fogh Odgaard * **Jakob Stoustrup** **

* *Department of Electronic Systems, Aalborg University, 9220 Aalborg East, Denmark (e-mail: pfo@es.aau.dk).*
** *Department of Electronic Systems, Aalborg University, 9220 Aalborg East, Denmark*

Abstract: Reliability and sustainability of wind turbines increase in importance as wind turbines contribute with increasing power generation to the world's power grids. One possible way to achieve this is by using advanced fault detection and isolation methods in wind turbines based on the measurements provided to the control system. In this paper a Karhunen-Loeve basis approach is designed for detecting changes in frequency response from rotating parts like a gearbox. The potential of this method is shown by applying it to an established Wind Turbine FDI and FTC Benchmark model. These faults are industrial wind turbines detected using auxiliary condition monitoring systems, which uses their own sensors etc. Usage of the existing control system including sensors will thereby provide a potential cost reduction of the wind turbine.

Keywords: Wind turbine, Fault Detection, Karhunen-Loeve basis.

1. INTRODUCTION

Wind turbines play a rapidly increasing role in the world's power grids. Consequently reliability of these turbines are of increasing importance both from a grid stability point-of-view and from a cost of energy perspective. Usages of modern fault detection, isolation and accommodation methods are one of the approaches which can be used to achieve this.

The predominant industrial approach for fault detection and accommodation in wind turbines is at present to use simple fault detection methods applied to the available control system sensor signals, like thresholds on measurements, and as well condition monitoring systems used on some of the expensive rotating parts like gearboxes and bearings. These condition monitoring systems are using additional, often expensive measurements of accelerations and vibrations or sound. More information on wind turbine condition monitoring can be found in Hameed et al. [2010] and Yang et al. [2010]. It is consequently an expensive add-on to the control system. Reviews of wind turbine condition monitoring can be found in Amirat et al. [2009], Hameed et al. [2009] and Garcia Marquez et al. [2012]. It would clearly be beneficial if one could use the measurements available in the control system to detect changes in the condition of e.g. the gearbox in a wind turbine. To facilitate research for this problem a friction change in the drive train gearbox was included in the wind turbine fault detection, isolation and accommodation benchmark model proposed by the same authors in Odgaard et al. [2009], in which the parameters in the 3 state gearbox model change slightly both in frequency and damping coefficient.

A wind turbine converts wind energy to electrical energy. The state-of-the-art wind turbine is an up wind three bladed turbine. Three blades are mounted on a rotor shaft and the wind force are converted into torque on the rotor shaft by acting on the blades. This torque can be controlled by pitching the blades or by controlling the generator torque. In between the rotor axis and the electrical generator, normally a gearbox is mounted, converting the low speed high torque rotor side with the high speed low torque generator side. For more details on turbines consult Bianchi et al. [2007] and Burton et al. [2008]. The generator speed measurement will contain a frequency component due to the gearbox resonance frequencies. These might be lowered with the usage of a drive train damper, which will move a part of this component to the generator torque control signal. An example of a drive train damper can be seen in Licari et al. [2012]. It could consequently be relevant to detect condition changes in the gearbox by monitoring changes in frequency content of the generator speed measurement and/or the generator torque control signal. A number of published approaches have been applied to the previously mentioned benchmark model. Some of these contributions are evaluated in Odgaard et al. [2013]. Others of these contributions can be seen in Chen et al. [2011], Laouti et al. [2011], Ozdemir et al. [2011], Svard and Nyberg [2011], Zhang et al. [2011], Pisu and Ayalew [2011], Blesa et al. [2011], Dong and Verhaegen [2011], Kiasi et al. [2011], Simani et al. [2011a], Simani et al. [2011b] and Stoican et al. [2011]. To the knowledge of the authors none of these or other contributions to wind turbine fault detection and isolation have taken the approach of detecting frequency change in the generator speed sensor signal to detect condition changes in the gearbox, or did not have any success using other methods for detecting this. In Odgaard and Stoustrup [2013] a frequency based scheme for detecting this gearbox fault is presented. This approach detects changes in the gearbox

resonance frequency by using a band pass filter at the gearbox resonance frequency.

Since the involved signals have both temporal and frequency characteristics, this problem requires a time-frequency basis solution in which there is support in both time and frequency. A simple first approach would be check if the frequency spectrum has changed. It is especially important to notice that the entire frequency spectrum does not require to be assessed, but only the part in which the drive train dynamics are present. It might not be so simple that a resonance frequency just changes to the fault or the amplitude of a resonance change. In this work a basis approximating the general trends of the original fault free frequency spectrum is found by extracting a Karhunen-Loeve basis from a windowed FFT of fault free data. Details on the Karhunen-Loeve basis can be found in Wickerhauser [1994] and Mallat [1999]. Examples of using Karhunen-Loeve basis for fault detection can be found in Odgaard et al. [2006] and Odgaard and Wickerhauser [2007]. This approximating basis supports the general trends in the frequency spectrum. The gearbox fault can subsequently be detected by comparing relative energy content in the component supported by the approximating basis relatively to the entire energy content in the given window at which the FFT was performed.

In Sec. 2 the system and fault in question are described, which is the gearbox resonance frequency change in the FDI wind turbine benchmark model presented in Odgaard et al. [2009]. The proposed scheme is presented in Sec. 3, followed by simulations and evaluations of the proposed scheme in Sec. 4. The paper is finalized by a conclusion in Sec. 5.

2. SYSTEM DESCRIPTION

This paper considers a generic wind turbine of 4.8 MW described in Odgaard et al. [2009]. The benchmark model contains 9 different faults, of which the gearbox fault is one. In this paper only the gearbox fault is considered. This turbine is a variable speed three blade pitch controlled turbine, with a front horizontal axis rotor.

2.1 Wind Turbine Model

The used wind turbine model is a benchmark model presented originally in Odgaard et al. [2009] and in additional details in Odgaard et al. [2013]. The details can be found in the mentioned paper, and are not described in full in the present paper. An overview of the model can be seen in Fig. 1, in which v_w denotes the wind speed, τ_r denotes the rotor torque, ω_r denotes the rotor speed, τ_g denotes the generator torque, ω_g denotes the generator speed, β_r denotes the pitch angle control reference, β_m denotes the measured pitch angles, $\tau_{w,m}$ denotes the estimated rotor torque, $\omega_{r,m}$ denotes the measured rotor speed, $\tau_{g,m}$ denotes the measured generator torque, $\omega_{g,m}$ denotes the measured generator speed, P_g denotes the measured generated electrical power, $\tau_{g,r}$ denotes the generator torque reference, and P_r denotes the power reference. The figure shows the relationship between the different model parts, which are described in the following text. They are Blade and Pitch System, Drive Train, Converter and Generator, and Controller. In addition the wind and sensors are modeled.

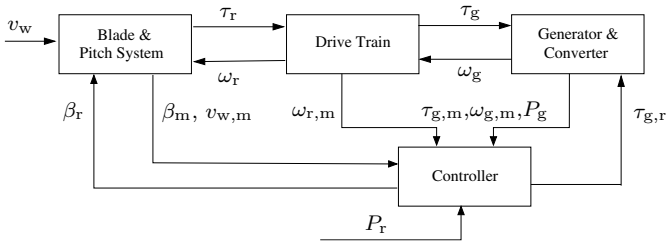

Fig. 1. This figure shows an overview of the benchmark model. It consists of four parts: Blade and Pitch Systems, Drive Train, Generator & Converter, and Controller. The variables in the figure are defined in text.

Each element of the model is shortly described in the following.

Wind Model The wind speed is given by a wind model including mean wind trends, turbulence, wind shear and tower shadow.

Aerodynamic and Pitch Actuator Model Aerodynamics and pitch actuators are modeled in the Blade and Pitch System model. The pitch actuator is modeled as a second order transfer function with constraints. The aerodynamics are modeled by a static mapping from the pitch angle, rotor and wind speeds to the torque acting on the wind turbine rotor.

Drive Train Model The drive train, which is used to increase the speed from rotor to generator, is modeled with a flexible two-mass system. The drive train model includes the inertia of the rotor (which includes blades and the main shaft) and generator.

Converter Model The converter which controls the generator torque is modeled by a first order system with constraints. This model covers both the electrical behavior of the generator and converter.

Sensor Models This part of the model is not shown on the figure, since models of each sensor in the figure are included in the relevant part model. The model contains a number of sensors, generator and rotor speed, pitch angles, wind speed, converter torque, electrical power. All the sensors are modeled as the measured variable added with random noise.

Controller The wind turbine operates in principle in 4 regions: Region 1 in which wind speeds are too low for the wind turbine to operate, Region 2 in which the turbine operates up to a nominal wind speed (partial load), Region 3 between nominal and rated wind speed, where the nominal power can be produced, Region 4 above rated wind speed, where the wind turbine is closed down in order to limit extreme loads on the wind turbine.

The controller is active in Region 2 & 3. In Region 2, the optimal rotor speed is obtained by using the converter torque as control signal. In Region 3 the rotor speed is kept at a given reference value by pitching the blades, (the

converter keeps the power at the reference taking care of fast variations in the speed). The basic controller in the different regions is described in Johnson et al. [2006].

3. KARHUNEN-LOEVE BASIS BASED DETECTION SCHEME

The Karhunen-Loeve basis provides a basis with basis vectors ordered in respect to their approximating capacity of a given data set. The basis vectors are generated and sorted in such a way that the first basis vector supports much of the energy in the data set. This means the remaining basis vectors supports the differences from each sequence in the data set, see Wickerhauser [1994]. Consequently this basis can be used to compare the general trends in different data sequences. In this approach the trends approximated are found in the frequency domain, and consequently an FFT algorithm is applied to the data set before the Karhunen-Loeve basis is computed. This formed basis can be used to detect changes in the general trends in the frequency domain.

Define a matrix $\mathbf{X}$ of u column vectors in $\mathcal{R}^m$, where $u > m$, the Karhunen-Loeve basis minimizes the average linear approximation error of the column vectors in $\mathbf{X}$. In this scheme $\mathbf{X}$ is constructed by vectors, x_i , with the absolute values of the FFT of the data vectors of length m. The low frequency part of the FFT is not of interest since it contains dynamics from the rotation of the wind turbine and other resonances like the tower. The high frequency part is not if interest, since it does not contain the relevant resonances. Consequently only a part of the frequency range in the FFT is included in the x_i vector. The frequency range used is bounded by the lower frequency denoted as f_l and the upper frequency denoted as f_u.

A given vector x_i can be found from the measured data vector, y_i as follows.

- Compute the FFT of y_i, $y_{\text{fft},i}(f) = \text{fft}(y_i)$
- Set x_i as $x_i = [y_{\text{fft},i}(f_l) \ \cdots \ y_{\text{fft},i}(f_u)]^T$.

The Karhunen-Loeve basis $\mathcal{K}$ is defined as

$$\mathcal{K} = \{v_1, \cdots, v_m\}, \tag{1}$$

which is an orthonormal basis of eigenvectors of $\mathbf{X}\mathbf{X}^T$, ordered in such a way that v_n is associated with the eigenvalue λ_n, and $\lambda_i \leq \lambda_j$ for $i \leq j$. This means that a basis, $\mathbf{K}_\text{L}$ of the the l most approximating basis vectors can be defined as

$$\mathbf{K}_\text{L} = \{v_m, v_{m-1}, \cdots, v_{m-l+1}\}. \tag{2}$$

Now the approximating Karhunen-Loeve is found, the coefficients, κ_i, for these vectors can be found for a given data vector y_i.

- Compute the FFT of y_i, $y_{\text{fft},i}(f) = \text{fft}(y_i)$
- Set x_i as $x_i = [y_{\text{fft},i}(f_l) \ \cdots \ y_{\text{fft},i}(f_u)]^T$.
- Compute κ_i as $\kappa_i = x_i^T \cdot \mathbf{K}_\text{L}$.

The approximation of x_i, denoted as $\bar{x}_i$ is subsequently computed as

$$\bar{x}_i = \mathbf{K}_L \cdot \kappa_i^T. \tag{3}$$

The last part of this detection scheme is to determine the ratio, $\gamma[n]$, of energy supported by the $\mathbf{K}_L$ basis relatively to the energy in $y_{\text{fft},i}$.

$$\gamma[n] = \frac{\bar{x}_i^T \cdot \bar{x}_i}{y_{\text{fft},i}^T \cdot y_{\text{fft},i}}. \tag{4}$$

$\gamma[n]$ is computed for each sample n, and this ratio will drop if relative energy content in the approximated frequencies, at which it is expected that the gearbox will have an energy content, are decreasing due to a changed dynamic behavior of the drive train.

This proposed scheme is somewhat computationally demanding since a FFT is required to be computed for each time each of a window length, L, where L should be so large that a reasonable frequency resolution in the interval between f_l and f_u is present. It is not necessarily a problem that this scheme is computationally demanding, since changes in the gearbox resonance will occur slowly over time, so the computations do not have to be executed for each sample. Instead they can be computed with a much slower frequency, but using data with the original sample frequency in order to obtain a high enough frequency resolution.

4. SIMULATION AND EVALUATION OF THE PROPOSED SCHEME

The Karhunen-Loeve basis is computed based on data from the benchmark model without gearbox fault present. The proposed detection scheme presented in Sec. 3, includes a number of parameters which can be adjusted in the tuning process. The window length used in the FFT computation is set to 2000, the frequency range for which the Karhunen-Loeve basis is found is given by $f_l = 2$ Hz and $f_u = 6$ Hz, and since the sample frequency is 100 Hz, the frequency resolution in the $\mathbf{K}_L$ basis is equal to $\frac{100 \text{ Hz}}{2000} = 0.05$ Hz.

In these simulations the wind speed sequence from the benchmark model is used, and this wind sequence is plotted in Fig. 2.

The five most approximating basis vectors, $\{v_{m-4}, \cdots, v_m\}$, can be seen in Fig. 4. The coefficients in these vectors, $\{\kappa_{m-4}, \cdots, \kappa_m\}$ are shown in Fig. 4. This shows that the best potential for detection is by using the fourth most approximating basis vector, i.e. $l = 3$. This also means that $\gamma[n]$ is computed based on $\kappa_{m-3}[n]$ only.

Fault 9 which changes the gearbox resonance frequency occurs from 4000 s. The computed value of $\gamma[n]$ is plotted, see Fig. 5 for the time interval from 3400 s to 4300 s in order to ensure that the wind turbine is operating in the full power mode, and that the fault is present in a part of the interval.

From Fig. 5 it can be seen that $\gamma[n]$ clearly drops when the gearbox resonance frequency changes at 4000s with a delay on approximately 10 s. Based on the same test sequence the value of σ can be found. It seems that $\sigma = 0.25$ provides the best tradeoff between detection delay and

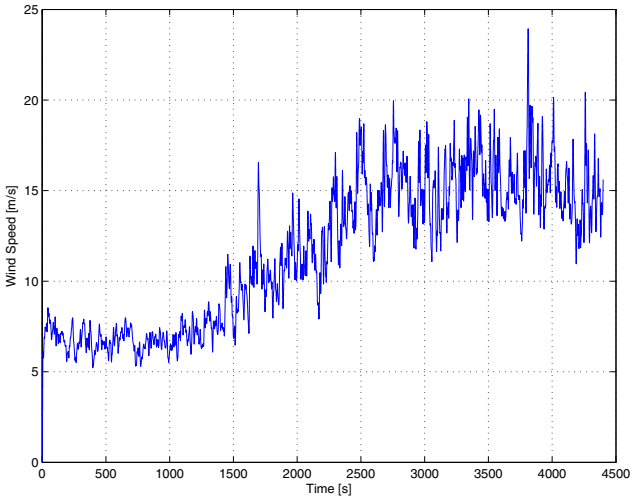

Fig. 2. Plot of wind speed sequence used in the benchmark model.

avoidance of false positive detections. The detection can be seen in Fig. 6 for the time interval 3400s-4300s.

It can be seen from test that the proposed scheme has a clear detection of the gearbox fault, it is a bit slow but quite robust to different operational conditions, in terms of avoiding potential false positive detections since the $\gamma[n]$ has a clear distinctive reaction during the fault. These initial tests clearly shows a potential of detecting gearbox faults using existing rotational speed measurements from the wind turbine control system, and thereby a possible cost reduction by monitoring the gearbox condition from the control system without additional sensors.

4.1 Further Work

The next natural step would be to test the proposed scheme on a more detailed model of the wind turbine gearbox without and with faults, which is operated in a realistic wind turbine simulation. Examples on such model and simulations can be seen in Nejad et al. [2012] and Nejad and Moan [2012].

It would also be relevant to perform this scheme on multiple sensors and actuator signals, e.g. it is relevant to include the generator torque reference in the drive train resonance frequency case considered in this work, since this would suppress variations in the generator speed in partial load operations, and thereby dampen the gearbox forces.

5. CONCLUSION

In this paper a scheme for detecting changes in a wind turbine gearbox is presented. This scheme is applied to the generator speed measurement from a benchmark wind turbine model, and the scheme is based on a Karhunen-Loeve basis which supports the general trends in the generator speed in frequency domain. Since the frequency domain of the generator speed changes during a gearbox fault, this can be detected using this trend approximating basis. The proposed scheme is tested on a known wind turbine FDI and FTC Benchmark Model. This test shows a potential of the proposed scheme for detecting gearbox

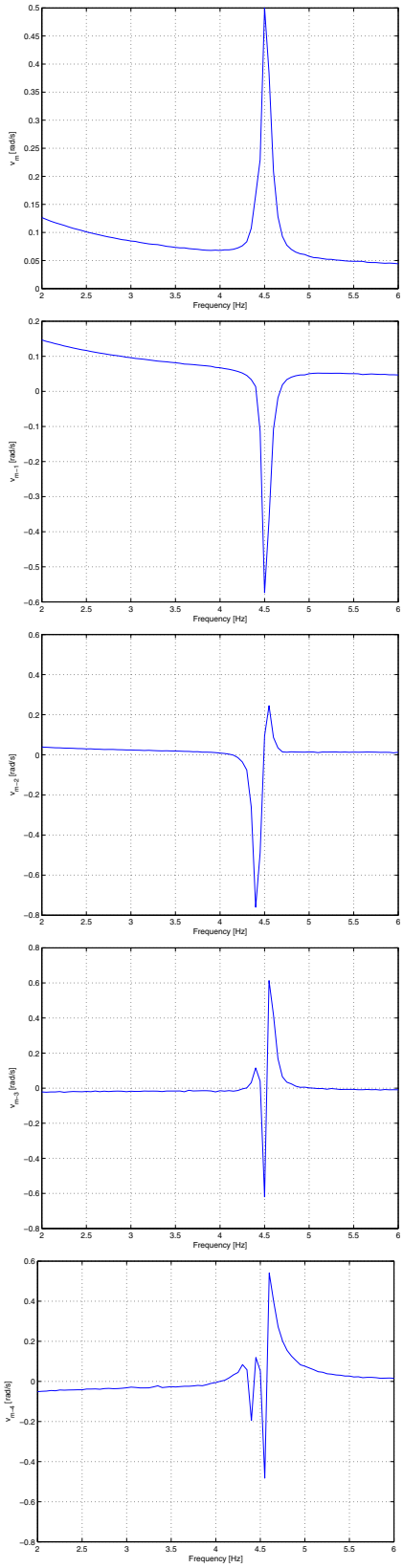

Fig. 3. Plot of the five most approximating Karhunen-Loeve basis vectors, v_{m-4} - v_m.

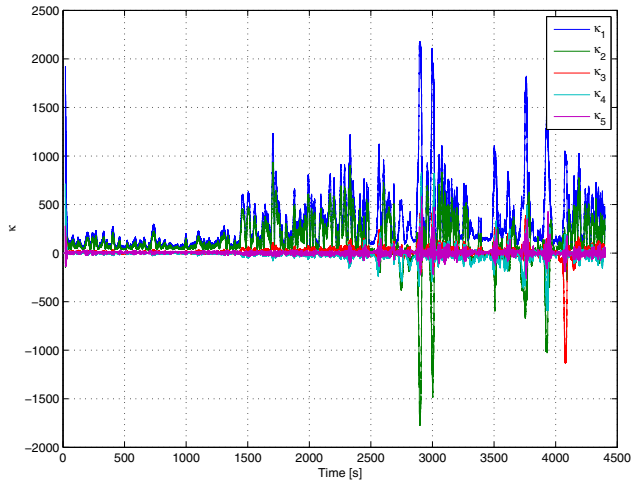

Fig. 4. $\{\kappa_{m-4}, \cdots, \kappa_m\}$ the coefficients in the five most approximating basis vectors.

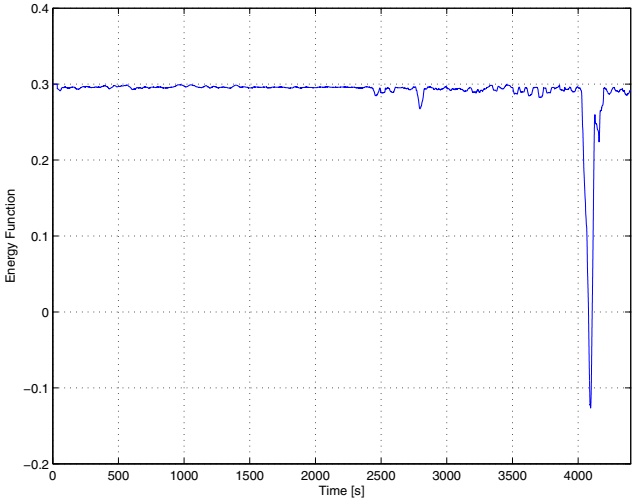

Fig. 5. A zoom on $\gamma[n]$ for the time interval 3400s to 4300s.

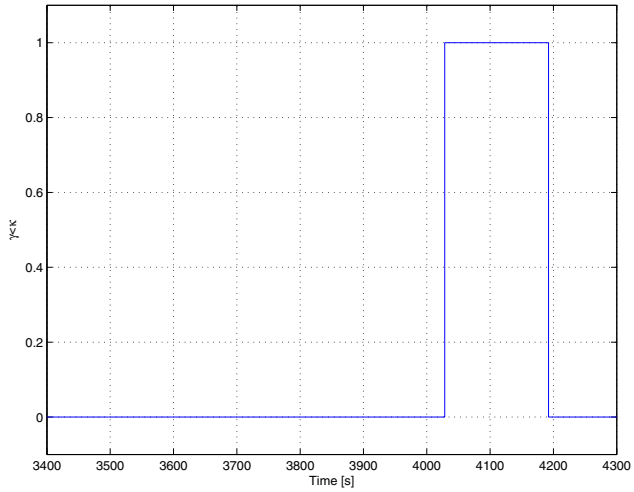

Fig. 6. A zoom on the detection based on $\gamma[n] < \sigma$ for the time interval 3400s to 4300s.

faults. This enables the possibility of using generator and rotor speed measurements for gearbox fault detection in wind turbines, and thereby reducing costs by removing the need for expensive auxiliary condition monitoring systems.

REFERENCES

Y. Amirat, M.E.H. Benbouzid, E. Al-Ahmar, B. Bensaker, and S. Turri. A brief status on condition monitoring and fault diagnosis in wind energy conversion systems. *Renewable and Sustainable Energy Reviews*, 2009. doi: 10.1016/j.rser.2009.06.031.

F.D. Bianchi, H. De Battista, and R.J. Mantz. *Wind Turbine Control Systems*. Advances in Industrial Control. Springer Verlag, London, 2007.

J. Blesa, V. Puig, J. Romera, and J. Saludes. Fault diagnosis of wind turbines using a set-membership approach. In *Proceedings of IFAC World Congress 2011*, pages 8316–8321, Milan, Italy, August-September 2011. doi: 10.3182/20110828-6-IT-1002.01167.

T. Burton, D. Sharpe, N. Jenkins, and E. Bossanyi. *Wind Energy Handbook*. Wiley, Chichester, UK, 6th edition, January 2008.

W. Chen, S.X. Ding, A.H.A. Sari, A. Naik, A.Q. Khan, and S. Yin. Observer-based FDI schemes for wind turbine benchmark. In *Proceedings of IFAC World Congress 2011*, pages 7073–7078, Milan, Italy, August-September 2011. doi: 10.3182/20110828-6-IT-1002.03469.

J. Dong and M. Verhaegen. Data driven fault detection and isolation of a wind turbine benchmark. In *Proceedings of IFAC World Congress 2011*, pages 7086–7091, Milan, Italy, August-September 2011. doi: 10.3182/20110828-6-IT-1002.00546.

F.P. Garcia Marquez, A.M. Tobias, J.M. Pinar Perez, and M. Papaelias. Condition monitoring of wind turbines: Techniques and methods. *Renewable Energy*, 46(1):169–178, October 2012. doi: 10.1016/j.renene.2012.03.003.

Z. Hameed, Y.S. Hong, Y.M. Cho, S.H. Ahn, and C.K. Song. Condition monitoring and fault detection of wind turbines and related algorithms: A review. *Renewable and Sustainable Energy Reviews*, 13(1):1–39, January 2009. doi: 10.1016/j.rser.2007.05.008.

Z. Hameed, S.H. Ahn, and Y.M. Cho. Practical aspects of a condition monitoring system for a wind turbine with emphasis on its design, system architecture, testing and installation. *Renewable Energy*, 5(5):879–894, 2010. doi: 10.1016/j.renene.2009.10.031.

K.E. Johnson, M.J.. Pao, L.Y.and Balas, and L.J. Fingersh. Control of variable-speed wind turbines - standard and adaptive techniques for maximizing energy capture. *IEEE Control Systems Magazine*, 26(3):71–81, June 2006. doi: 10.1109/MCS.2006.1636311.

F. Kiasi, J. Prakash, S. Shah, and J.M. Lee. Fault detection and isolation of benchmark wind turbine using the likelihood ratio test. In *Proceedings of IFAC World Congress 2011*, pages 7079–7085, Milan, Italy, August-September 2011. doi: 10.3182/20110828-6-IT-1002.03535.

N. Laouti, N. Sheibat-Othman, and S. Othman. Support vector machines for fault detection in wind turbines. In *Proceedings of IFAC World Congress 2011*, pages 7067–7072, Milan, Italy, August-September 2011. doi: 10.3182/20110828-6-IT-1002.02560.

J. Licari, C.E. Ugalde-Loo, J. Ekanayake, and N. Jenkins. Comparison of the performance of two torsional vibration dampers considering model uncertainties and parameter variation. In *Proceedings of EWEA 2012*, Copenhagen, Denmark, April 2012.

S. Mallat. *A wavelet tour of signal processing*. Academic Press, 2nd edition, 1999.

A.R. Nejad and T. Moan. Effect of geometrical imperfections of gears in large offshore wind turbine gear trains: 0.610 mw case studies. In *Proceedings of EWEA 2012*, Copenhagen, Denmark, April 2012.

A.R. Nejad, Y. Xing, and T. Moan. Gear train internal dynamics in large offshore wind turbines. In *Proceedings of the ASME 2012 11th Biennial Conference On Engineering Systems Design And Analysis ESDA2012*, pages 1–9, Nates, France, July 2012.

P. F. Odgaard and M. V. Wickerhauser. Karhunen-loevve (pca) based detection of multiple oscillations in multiple measurement signals from large-scale process plants. In *Proc. American Control Conference ACC '07*, pages 5893–5898, 9–13 July 2007. doi: 10.1109/ACC.2007.4282149.

P.F. Odgaard and J. Stoustrup. Frequency based fault detection in wind turbines. In *Submitted for conference publication*, 2013.

P.F. Odgaard, J. Stoustrup, P. Andersen, M.V. Wickerhauser, and H.F. Mikkelsen. A fault tolerant control scheme for CD players to handle surface defects. *Control Engineering Practice*, 14(12):1495–1509, December 2006. doi: 10.1016/j.conengprac.2006.01.002.

P.F. Odgaard, J. Stoustrup, and M. Kinnaert. Fault tolerant control of wind turbines - a benchmark model. In *Proceedings of the 7th IFAC Symposium on Fault Detection, Supervision and Safety of Technical Processes*, pages 155–160, Barcelona, Spain, June-July 2009. IFAC. doi: 10.3182/20090630-4-ES-2003.0090.

P.F. Odgaard, J. Stoustrup, and M. Kinnaert. Fault tolerant control of wind turbines - a benchmark model. *IEEE Transactions on Control System Technology*, 21(4):1168–1182, July 2013. doi: 10.1109/TCST.2013.2259235.

A.A. Ozdemir, P. Seiler, and G.J. Balas. Wind turbine fault detection using counter-based residual thresholding. In *Proceedings of IFAC World Congress 2011*, pages 8289–8294, Milan, Italy, August-September 2011. doi: 10.3182/20110828-6-IT-1002.01758.

P. Pisu and B. Ayalew. Robust fault diagnosis for a horizontal axis wind turbine. In *Proceedings of IFAC World Congress 2011*, pages 7055–7060, Milan, Italy, August- September 2011. doi: 10.3182/20110828-6-IT-1002.02540.

S. Simani, P. Castaldi, and M. Bonfe. Hybrid model-based fault detection of wind turbine sensors. In *Proceedings of IFAC World Congress 2011*, pages 7061–7066, Milan, Italy, August-September 2011a. doi: 10.3182/20110828-6-IT-1002.01311.

S. Simani, P. Castaldi, and A. Tilli. Data-driven approach for wind turbine actuator and sensor fault detection and isolation. In *Proceedings of IFAC World Congress 2011*, pages 8301–8306, Milan, Italy, August-September 2011b. doi: 10.3182/20110828-6-IT-1002.00447.

F. Stoican, C.-F. Raduinea, and S. Olaru. Adaptation of set theoretic methods to the fault detection of wind turbine benchmark. In *Proceedings of IFAC World Congress 2011*, pages 8322–8327, Milan, Italy, August-September 2011. doi: 10.3182/20110828-6-IT-1002.01842.

C. Svard and M. Nyberg. Automated design of an FDI-system for the wind turbine benchmark. In *Proceedings of IFAC World Congress 2011*, pages 8307–8315, Milan, Italy, August-September 2011. doi: 10.3182/20110828-6-IT-1002.00618.

M.V. Wickerhauser. *Adapted Wavelet Analysis from Theory to Software*. A K Peters, Ltd., 1st edition, 1994.

W. Yang, P.J. Tavner, C.J. Crabtree, and M. Wilkinson. Cost-effective condition monitoring for wind turbines. *IEEE Transactions on Industrial Electronics*, 57(1):263–271, January 2010. doi: 10.1109/TIE.2009.2032202.

X. Zhang, Q. Zhang, S. Zhao, R. M.G. Ferrari, M. M. Polycarpou, and T. Parisini. Fault detection and isolation of the wind turbine benchmark: An estimation-based approach. In *Proceedings of IFAC World Congress 2011*, pages 8295–8300, Milan, Italy, August-Septemper 2011. doi: 10.3182/20110828-6-IT-1002.02808.